

patient on ^{99m}Tc -ECD SPECT was thought to exclude HSE. The expected hyperactivity of the temporal lobe was seen when the patient was reevaluated with ^{99m}Tc -HMPAO.

Technetium-99m-ECD and ^{99m}Tc -HMPAO are both lipophilic agents that penetrate the normal blood-brain barrier. Both are retained by conversion of the lipophilic molecule into hydrophilic compounds. Technetium-99m-ECD is hydrolyzed to polar metabolites by deesterification (10). The decrease of ^{99m}Tc -ECD activity on dynamic SPECT of our patient indicates the absence or reduction of this enzymatic process in the inflammatory lesion of HSE. The resulting lack of retention causes the pathologic area to appear hypoactive despite the initial presence of hyperperfusion.

Similar observations have been made in the subacute phase of an ischemic stroke where ^{99m}Tc -ECD was noted to miss reflow hyperemia (4,5). In such a setting, this need not constitute a significant disadvantage as the failure to achieve the enzymatic transformation of ^{99m}Tc -ECD may be a better indicator of the extent of tissue damage and prognosis than the visualization of hyperemia (5,11). The inability to detect hyperemia with ^{99m}Tc -ECD in the presence of cellular dysfunction must be viewed differently when considering HSE. Routinely performed dynamic data collection can reduce this problem, but these images have limited resolution and may not be available.

CONCLUSION

Dynamic acquisition following the administration of ^{99m}Tc -HMPAO, ^{123}I -IMP or ^{99m}Tc -ECD demonstrates regional hyperemia of the temporal lobe in HSE. Technetium-99m-ECD, how-

ever, washes out. Consequently, hyperemia characteristic of HSE is not detected in clinical SPECT images acquired 2 min later.

REFERENCES

1. Devous MD, Sr, Payne JK, Lowe JL, Leroy RF. Comparison of technetium-99m-ECD to Xenon-133 SPECT in normal controls and in patients with mild to moderate regional cerebral blood flow abnormalities. *J Nucl Med* 1993;34:754-761.
2. Léveillé J, Demonceau G, Walovitch RC. Intrasubject comparison between technetium-99m-ECD and technetium-99m-HMPAO in healthy human subjects. *J Nucl Med* 1992;33:480-484.
3. Pupi A, Castagnoli A, De Cristofaro MTR, Bacciottini L, Petti AR. Quantitative comparison between ^{99m}Tc -HMPAO and ^{99m}Tc -ECD: measurement of arterial input and brain retention. *Eur J Nucl Med* 1994;21:24-130.
4. Lassen NA, Sperling B. Technetium-99m-bicisate reliably images CBF in chronic brain diseases but fails to show reflow hyperemia in subacute stroke: report of a multicenter trial of 105 cases comparing ^{133}Xe and ^{99m}Tc -bicisate (ECD, Neurolite) measured by SPECT on same day. *J Cereb Blood Flow Metab* 1994;14(suppl 1):S44-S48.
5. Tsuchida T, Nishizawa S, Yonekura Y, et al. SPECT images of technetium-99m-ethyl cysteinate dimer in cerebrovascular diseases: comparison with other cerebral perfusion tracers and PET. *J Nucl Med* 1994;35:27-31.
6. Launes J, Nikkinen P, Lindroth L, Brownell A, Liewebdahl K, Iivanainen M. Diagnosis of acute herpes simplex encephalitis by brain perfusion single photon emission computed tomography. *Lancet* 1988;2:1188-1191.
7. Schmidbauer M, Podreka I, Wimberger D, et al. SPECT and MR imaging in herpes simplex encephalitis. *J Comput Assist Tomogr* 1991;15:811-815.
8. McEwan JR, Park CH, Kim SM, et al. Technetium-99m exametazime brain SPECT and magnetic resonance images in the diagnosis of herpes simplex encephalitis. *Clin Nucl Med* 1994;19:66-68.
9. Kao CH, Wang SJ, Mak SC, Shian WJ, Chi CS. Viral encephalitis in children: detection with technetium-99m HMPAO brain single-photon emission CT and its value in prediction of outcome. *Am J Neuroradiol* 1994;15:1369-1373.
10. Walovitch RC, Hill TC, Garrity ST, et al. Characterization of technetium-99m-L,L-ECD for brain perfusion imaging. Part 1: pharmacology of technetium-99m-ECD in nonhuman primates. *J Nucl Med* 1989;30:1892-1901.
11. Brass LM, Walovitch RC, Joseph JL, et al. The role of single-photon emission computed tomography brain imaging with ^{99m}Tc -bicisate in the localization and definition of mechanism of ischemic stroke. *J Cereb Blood Flow Metab* 1994;14(suppl 1):S91-S98.

Reproducibility of the Distribution of Carbon-11-SCH 23390, a Dopamine D₁ Receptor Tracer, in Normal Subjects

Grace L.-Y. Chan, James E. Holden, A. Jon Stoessl, Doris J. Doudet, Yue Wang, Teresa Dobko, K. Scott Morrison, Joe M. Huser, Carolyn English, Barbara Legg, Michael Schulzer, Donald B. Calne and Thomas J. Ruth
TRIUMF and Neurodegenerative Disorders Centre, University of British Columbia, Vancouver, British Columbia, Canada; and Department of Medical Physics, University of Wisconsin, Madison, Wisconsin

The reproducibility of [^{11}C]SCH 23390 in PET was studied in 10 normal human subjects. **Methods:** The scan-to-scan variation of several measures used in PET data analysis, including the radioactivity ratio, plasma-input Logan total distribution volume (DV), plasma-input Logan DV ratio (DVR) and tissue-input Logan $B_{\text{max}}/K_{\text{d}}$ values, was determined. **Results:** There were significant correlations among the radioactivity ratio, plasma-input DVR and tissue-input $B_{\text{max}}/K_{\text{d}}$. With the cerebellum as the reference region, these three measures also had high reliability (86%–95%), high between-subject s.d. (7.7%–11.3%) and small within-subject s.d. (2.3%–3.6%), indicating that they are comparable and useful measures for the assessment of dopamine D₁ receptor binding. **Conclusion:** The radioactivity ratio and the tissue-input $B_{\text{max}}/K_{\text{d}}$ may be preferred methods for the evaluation of dopamine D₁ receptor binding because these two methods do not require arterial blood sampling and

metabolite analysis. Our results show that cerebellum is a reliable reference region for SCH 23390. When the Logan plasma-input function method is used in data analysis for SCH 23390, DVRs rather than total DV values should be used because of the poor reliability of the DV values and their lack of correlation with other measures. Carbon-11-SCH 23390 is thus a reliable and reproducible ligand for the study of dopamine D₁ receptor binding by PET.

Key Words: carbon-11-SCH 23390; PET imaging

J Nucl Med 1998; 39:792-797

The tracer [^{11}C]SCH 23390 is widely used as a ligand to study dopamine D₁ receptor function using PET (1-4). The binding of SCH 23390 to dopamine D₁ receptors, as determined by PET, can be assessed by several methods. The simplest method uses the ratio of activity in regions of high specific binding (such as striatum) to those of nonspecific binding (such as cerebellum). Another method measures the distribution volume (DV) of the ligand in specific and nonspecific regions of

Received May 2, 1997; revision accepted Aug. 6, 1997.

For correspondence or reprints contact: Grace L.-Y. Chan, PhD, Positron Emission Tomography, Room G343, Acute Care Unit, Vancouver Hospital and Health Sciences Center, University of British Columbia Site, 2211 Wesbrook Mall, Vancouver, British Columbia, Canada V6T 2B5.

interest (ROIs) and their ratio (5). Recently, a new method was proposed by Logan et al. (6) that yields an equivalent to the DV ratio (DVR) but without the need for a plasma input function. This approach uses the radioactivity time course in a nonspecific brain region as input function in the analysis of specific brain regions. The usefulness of these measures for the study of changes of dopamine D₁ receptor binding, either due to the normal aging process, progression of disease, pharmacologic intervention, therapeutic treatment or other factors, depends on their reproducibility. In this study, we performed repeat SCH 23390 PET scans in normal human subjects to measure scan-to-scan variation in the different measures used in data analysis. Either a cortical region or cerebellum is often used as a reference region to determine free and nonspecifically bound tracer in dopamine receptor studies because of the low number of dopamine receptors. In this study, we analyzed SCH 23390 PET data using both the cerebellum and occipital cortex as reference regions. Data were then compared to determine which region was most suitable using reliability as a metric.

MATERIALS AND METHODS

Chemistry

Carbon-11-SCH 23390 was synthesized by N-methylation of the desmethyl precursor analog (SCH 24518) using [¹¹C]methyl iodide (7). Carbon-11-methyl iodide was reacted with 1.5 mg of SCH 24518 (free-form salt) in 450 μl of dimethyl formamide. The reaction was performed in a dry ice/isopropanol bath for 5 min at 55°C with constant stirring. The product was then purified on a silica high-performance liquid chromatography (HPLC) column. Radiochemical yield was 50%–60%. The desmethyl precursor of SCH 23390 was supplied by Schering Plough Pharmaceutical Corporation (Bloomfield, NJ). The specific activity of [¹¹C]SCH 23390 was 448 ± 232 Ci/mmol (mean ± s.d.) (range 189–1189 Ci/mmol) at ligand injection, and the radiochemical purity was >99%.

Subjects

Ten normal subjects (6 men, 4 women; age range 22–74 yr; mean age ± s.d. = 50.5 ± 18.4 yr) participated in the study. None had neurologic disease by history or by clinical examination. Each subject was scanned twice, with the second scan taken between 3 and 10 wk after the first (39 ± 16 days). All subjects gave written informed consent before each scan. The study was approved by the University of British Columbia Human Ethics Committee.

PET Scans and Blood Sampling

PET scans were performed using an ECAT 953B/31 tomograph (Siemens, Knoxville, TN). The subject was positioned in the gantry using three laser lights to ensure the subject's head was centered in the field of view. A thermoplastic mask was then molded to the subject's head to restrain movement, and the same mask was used in repositioning for the second scan. Before injection of [¹¹C]SCH 23390, a transmission scan with ⁶⁸Ge rods was obtained for attenuation correction. SCH 23390 (228 ± 38 MBq in 10 ml of saline) was injected intravenously over 60 sec using a Harvard infusion pump. Arterial blood samples were obtained from the radial artery for measurement of total radioactivity and metabolite analysis. For assessment of total radioactivity, six arterial blood samples were collected during the first minute immediately after tracer injection, followed by another six samples in the second minute and at 3, 4, 5, 7, 10, 15, 20, 30, 40, 50 and 60 min thereafter. Additional arterial blood samples were collected at 3, 10, 20, 30 and 40 min and analyzed by HPLC to determine the percentage of unchanged ligand in plasma at these time points. The PET scan protocol included four 1-min, three 2-min, eight 5-min sequential

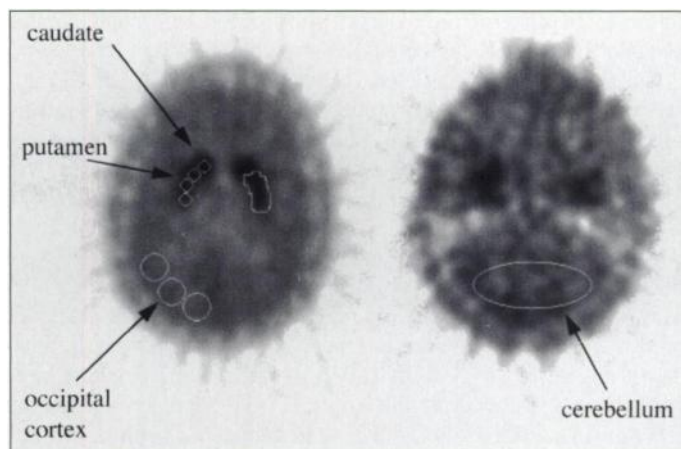


FIGURE 1. Typical placement of ROIs. (Left) Placement of one circular ROI on the caudate, three circular ROIs on the putamen, an irregularly shaped ROI on the whole putamen and three circular ROIs on the occipital cortex. (Right) Placement of one oval ROI on the cerebellum. The irregularly shaped ROI was drawn around the putamen on the summed image of the first subject and subsequently translocated on the other subjects.

emission scans and one 10-min sequential emission scan, starting at midpoint of tracer injection.

Metabolite Analysis by High-Performance Liquid Chromatography

A liquid chromatograph equipped with a Waters Model 510 pump (Millipore, Toronto, Ontario, Canada) and a Rheodyne, Inc. (Cotati, CA) model 7161 injector was used for HPLC analysis. A Nova-Pak™ C18 RCM reverse-phase column (10 cm × 8 mm, 4 μm; Waters) and a guard column (Guard-Pak, Millipore) were used. An equal volume of acetonitrile was added to 0.5 ml of plasma sample. The mixture was vibrated for 10 sec and centrifuged at 14,000 × g for 5 min. The supernatant was filtered through a 0.45-μm Millipore filter before HPLC analysis. The mobile phase was 0.01 M ammonium phosphate dibasic buffer:methanol (35:65). Chromatography was performed isocratically at a flow rate of 2.8 ml/min. Fractions (0.7 min/tube) of the HPLC eluent were collected by an automated fraction collector and counted for radioactivity in a gamma counter (Picker Spectroscaler, Cleveland, OH) with gamma ray events in the energy range of 400–625 keV being recorded. Carbon-11-SCH 23390 and its metabolites were eluted at 5.5 min (fractions 8–10) and 1.5 min (fractions 2–3), respectively.

The recovery of SCH 23390 from HPLC analysis was 96% ± 5%, and its recovery from solvent extraction was 92% ± 2%. The data from metabolite analysis were used to correct the total radioactivity time courses to obtain the time courses of unchanged SCH 23390 in plasma.

Data Analysis

For each scan, seven consecutive axial slices containing the striatum (caudate and putamen) were summed to produce a composite image. On this summed image, ROIs were placed over the left and right striatum as follows: one circular ROI on the caudate nucleus (CAU) (61 mm²) and three circular ROIs (61 mm²) on the putamen (PUT1). In addition, an irregularly shaped ROI (360 mm²) encompassing the whole putamen (PUT2) was placed over the left and right striatum (Fig. 1). For nonspecific background, three circular ROIs (297 mm²) were placed on the occipital cortex (OC) bilaterally. These ROIs were then applied to the summed seven slices of each of the 16 time frames. In addition to the occipital cortex, the cerebellum (CE) was also used as an alternate nonspecific background region. Two consecutive slices were summed, and one oval ROI (2107 mm²) was placed on the cerebellum of the summed image and then applied to the 16 time

frames. The time-activity curves for the left and right striatal, occipital cortex and cerebellar ROIs were obtained.

The same time-activity curves were averaged over all time frames from 30 to 60 min postinjection. These average values were used to generate values for radioactivity ratios. Ratios of the caudate nucleus to both the occipital cortex (CAU/OC) and the cerebellum (CAU/CE) and ratios of the putamen to the occipital cortex and cerebellum using the average of three small ROIs (PUT1/OC and PUT1/CE) or one large ROI (PUT2/OC and PUT2/CE) were obtained. Total (specific plus nonspecific) DVs using metabolite-corrected plasma time courses as the reference plasma input function were estimated for caudate (DV_{CAU}), putamen using three small ROIs (DV_{PUT1}), putamen using one large ROI (DV_{PUT2}), the occipital cortex (DV_{OC}) and the cerebellum (DV_{CE}). In addition, the DVRs were calculated using either the occipital cortex (DV_{CAU}/DV_{OC} , DV_{PUT1}/DV_{OC} and DV_{PUT2}/DV_{OC}) or the cerebellum (DV_{CAU}/DV_{CE} , DV_{PUT1}/DV_{CE} and DV_{PUT2}/DV_{CE}) as the reference region.

Furthermore, DVRs using the radioactivity time courses in the occipital cortex or cerebellum as the reference tissue input function were determined by the method of Logan et al. (6). Values of the kinetic rate constant k_2 required by this approach were evaluated by conventional compartmental fitting of the reference tissue time courses. Because our goal was to evaluate the reliability of this approach performed without measurements in blood, the mean values for k_2 (cerebellum = 0.10/min; occipital cortex = 0.061/min) were used in the calculations. Values of the binding potential B_{max}/K_d were derived from the formula $(DVR - 1)$ (6).

Statistical Analysis

A one-way analysis of variance (ANOVA) was performed to obtain the mean, between-subject s.d. (s.d.b.) and within-subject s.d. (s.d.w.). Confidence intervals for s.d.w. were calculated using chi-square distribution and the reliability coefficients (R values) were estimated as follows: $R = s.d.b.^2 / (s.d.b.^2 + s.d.w.^2)$ (8). The reliability coefficient indicates the reproducibility of the measurements over time because it measures the intraclass correlation, i.e., the correlation between two measurements observed in the same individual at different times.

For metabolite data, the ratios of metabolite to unchanged SCH 23390 were plotted against time, and linear correlation analysis was used to test the line fit and determine the slope. The slopes were also subjected to one-way ANOVA to obtain s.d.b., s.d.w. and R values.

The radioactivity ratios, plasma-input DVRs and tissue-input B_{max}/K_d values of caudate or putamen to occipital cortex were compared to the same measures with the cerebellum as the nonspecific binding region. The correlation coefficient (r) obtained from the least squares regression line was compared to the critical values at the 5% level of significance. To compare the different methods used in data analysis, all the measures were further subjected to linear regression by pairs.

For 3 of the 10 subjects, the axial positioning was inadequate, and as a result, no cerebellar planes were acquired. In general, two cerebellar planes are essential for a reliable assessment of cerebellar ROIs. Thus, the statistical analyses of all DVRs or radioactivity ratios derived from cerebellar time courses were performed with 7 rather than 10 subjects.

RESULTS

After intravenous injection of ^{11}C -SCH 23390, radioactivity in the arterial blood peaked rapidly followed by an exponential decline. The radioactivity appeared rapidly in the brain. Figure 2 shows the time-radioactivity curves of several brain regions, as well as the time courses of total and

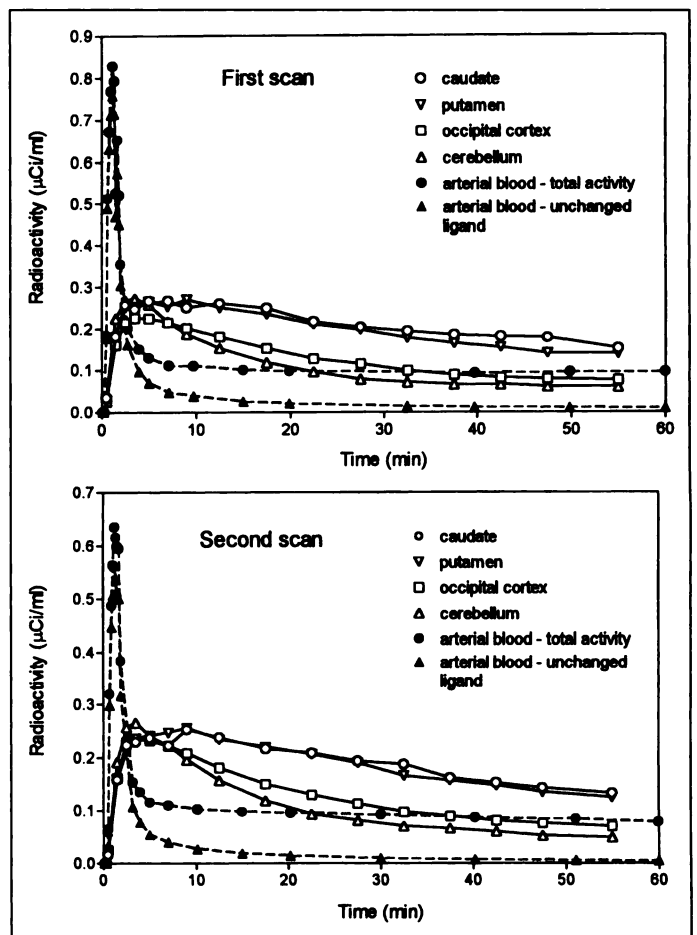


FIGURE 2 Time-activity curves of several brain regions of a normal human subject after receiving an intravenous injection of ~ 7 mCi of $[^{11}C]$ SCH 23390. The second scan (lower) was taken 3 wk after the first (upper). Also shown are the time courses of the total and unchanged ligand in the arterial blood.

unchanged ligand in the arterial blood of a representative subject.

The results of one-way ANOVA on the different measures for dopamine D_1 receptor binding, with either the occipital cortex or cerebellum as the nonspecific binding region, are shown in Table 1. Because paired Student's *t*-tests performed between the left and the right values of radioactivity ratios, total DV values, DVRs and B_{max}/K_d in both the first and second studies demonstrated no significant left/right differences, our data are presented as the average of both sides.

The radioactivity ratio of caudate or putamen to occipital cortex yielded a s.d.w. ranging from 3.4% to 4.4% of the group mean. The s.d.b. ranged from 6.8% to 8.2%, resulting in a reliability of 71% to 85%. The s.d.w., s.d.b. and reliability of the radioactivity ratio of caudate or putamen to cerebellum were 3.1%–3.6%, 7.9%–11.3% and 86%–91%, respectively.

For the total DV of caudate or putamen, the s.d.w. varied between 15.8% and 16.6% of the group mean, and the s.d.b. varied between 14.4% and 18.5%, resulting in a reliability of 43%–58%. The DVRs of caudate or putamen to occipital cortex gave a s.d.w. ranging from 3.3% to 4.4% of the group mean. The s.d.b. ranged from 6.6% to 8.0%, resulting in a reliability of 69%–86%. The s.d.w., s.d.b. and reliability for the DVRs of caudate or putamen to cerebellum were 2.8%–3.1%, 7.8%–10.7% and 86%–93%, respectively.

The B_{max}/K_d values using the occipital cortex as the tissue-input function gave a s.d.w. ranging from 3.1% to 4.2% of the group mean. The s.d.b. ranged from 6.0% to 7.5%, resulting in

TABLE 1

Results of a One-Way Analysis of Variance on Different Measures of Dopamine D₁ Receptor Binding

	Mean	s.d.b. (CV)	s.d.w. (CV)	95% CI	R values (%)
Radioactivity ratios					
CAU/OC	1.92	0.13 (6.8%)	0.08 (4.4%)	0.06–0.15	71
PUT1/OC	1.70	0.14 (8.2%)	0.06 (3.5%)	0.04–0.10	85
PUT2/OC	1.63	0.12 (7.5%)	0.06 (3.4%)	0.04–0.10	83
CAU/CE	2.67	0.21 (7.9%)	0.08 (3.1%)	0.06–0.17	86
PUT1/CE	2.33	0.26 (11.3%)	0.08 (3.6%)	0.06–0.17	91
PUT2/CE	2.22	0.23 (10.3%)	0.08 (3.6%)	0.05–0.16	89
Logan plasma-input DV and DVRs					
DV _{CAU}	7.42	1.37 (18.5%)	1.17 (15.8%)	0.82–2.06	58
DV _{PUT1}	6.56	0.95 (14.4%)	1.06 (16.1%)	0.74–1.86	44
DV _{PUT2}	6.35	0.92 (14.6%)	1.06 (16.6%)	0.74–1.85	43
DV _{OC}	4.20	0.70 (16.8%)	0.74 (17.5%)	0.51–1.29	48
DV _{CE}	3.58	0.64 (17.8%)	0.56 (15.7%)	0.39–0.98	56
DV _{CAU} /DV _{OC}	1.77	0.12 (6.6%)	0.08 (4.4%)	0.05–0.14	69
DV _{PUT1} /DV _{OC}	1.57	0.13 (8.0%)	0.05 (3.3%)	0.04–0.09	86
DV _{PUT2} /DV _{OC}	1.52	0.11 (7.1%)	0.05 (3.6%)	0.04–0.10	80
DV _{CAU} /DV _{CE}	2.20	0.17 (7.8%)	0.07 (3.1%)	0.05–0.14	86
DV _{PUT1} /DV _{CE}	1.91	0.20 (10.7%)	0.06 (2.9%)	0.04–0.11	93
DV _{PUT2} /DV _{CE}	1.85	0.18 (9.5%)	0.05 (2.8%)	0.03–0.11	92
Logan tissue-input B_{max}/K_d					
B _{max} /K _d (CAU/OC)	0.73	0.10 (6.0%)	0.07 (4.2%)	0.05–0.13	67
B _{max} /K _d (PUT1/OC)	0.55	0.12 (7.5%)	0.05 (3.1%)	0.03–0.08	85
B _{max} /K _d (PUT2/OC)	0.49	0.10 (6.6%)	0.05 (3.3%)	0.03–0.09	80
B _{max} /K _d (CAU/CE)	1.13	0.16 (7.7%)	0.06 (2.8%)	0.04–0.12	88
B _{max} /K _d (PUT1/CE)	0.88	0.20 (10.7%)	0.05 (2.6%)	0.03–0.10	95
B _{max} /K _d (PUT2/CE)	0.81	0.17 (9.6%)	0.04 (2.3%)	0.03–0.09	94

CV = coefficient of variation; 95% CI = 95% confidence interval; s.d.b. = between-subject s.d.; s.d.w. = within-subject s.d.; R = reliability coefficients.

a reliability of 67%–85%. The s.d.w., s.d.b. and reliability of the B_{max}/K_d values using the cerebellum as tissue-input function were 2.3%–2.8%, 7.7%–10.7% and 88%–95%, respectively.

Of all the measures analyzed, the reliability was about 6%–21% higher when the cerebellum instead of the occipital cortex was used as the reference region. The reliability was slightly higher (1%–6%) when three small ROIs instead of one large ROI were set on the putamen for data analysis, regardless of whether the occipital cortex or cerebellum was used as the reference region.

Figure 3 demonstrates the reproducibility of several extracted measures, presented as the values derived from the second scan plotted against those from the first scan. Data for the putamen (three small ROIs) are presented as representative examples. Derived measures include radioactivity ratios, plasma-input total DV, plasma-input DVRs and tissue-input B_{max}/K_d values. The cerebellum was used as the reference region.

Linear correlation analysis of the ratio of metabolite to unchanged SCH 23390 versus time yielded r values ranging from 0.935 to 0.997, with the slope being significantly different from zero (p < 0.05). The mean slopes were 0.23 ± 0.05 for the first study and 0.21 ± 0.07 for the second study (s.d.b. of 18.7%, s.d.w. of 22.7% and reliability of 40%).

There were significant correlations between the radioactivity ratios, plasma-input DVRs and tissue-input B_{max}/K_d values with occipital cortex as the nonspecific binding region and the same measures with the cerebellum as the nonspecific binding region. The correlation coefficient ranged from 0.808 to 0.976 (p = 0.0002–0.028).

Table 2 shows the results of linear regression analysis between the different measures when cerebellum was used as the reference region. There was a significant correlation (p < 0.05) between radioactivity ratios and plasma-input DVRs (r =

0.868–0.953). Similarly, there were significant correlations between radioactivity ratios and tissue-input B_{max}/K_d values (r = 0.905–0.956) and between plasma-input DVRs and tissue-input B_{max}/K_d values (r = 0.983–0.998). Similar signif-

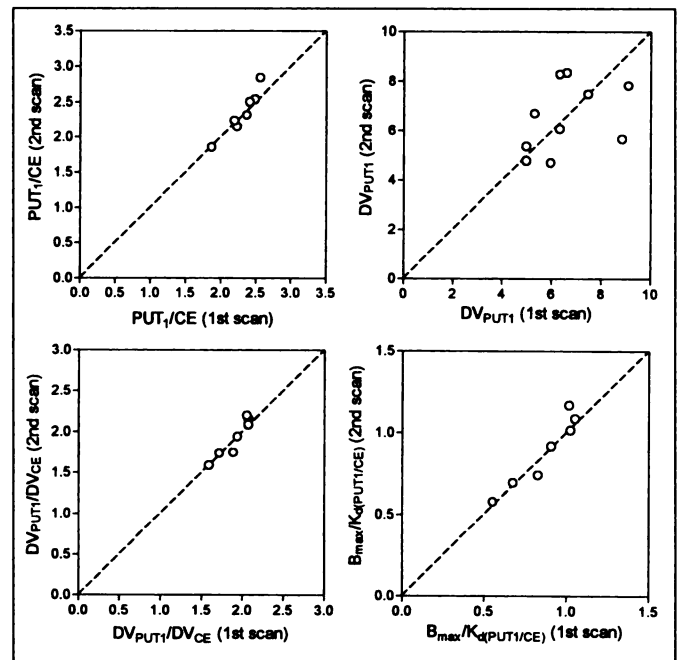


FIGURE 3. The reproducibility of several extracted measures are presented as the values derived from the second scan plotted against those from the first scan. Data for the putamen (three small ROIs) are presented as representative. Derived measures include radioactivity ratios, plasma-input total DVs, plasma-input DVRs and tissue-input B_{max}/K_d values. The cerebellum was used as the reference region. The dashed line is the perfect agreement lines between the values of the first and second scans.

TABLE 2
Linear Regression Analysis Between Different Measures of Dopamine D₁ Receptor Binding

	First scan		Second scan	
	r	p	r	p
Caudate nucleus				
CAU/CE versus DV _{CAU}	-0.571	0.241	-0.152	0.745
CAU/CE versus DV _{CAU} /DV _{CE}	0.868	0.011*	0.890	0.007*
CAU/CE versus B _{max} /K _d (CAU/CE)	0.907	0.005*	0.905	0.005*
DV _{CAU} versus B _{max} /K _d (CAU/CE)	-0.318	0.487	0.084	0.858
DV _{CAU} /DV _{CE} versus B _{max} /K _d (CAU/CE)	0.983	<0.0001*	0.986	<0.0001*
Putamen (with three ROIs)				
PUT1/CE versus DV _{PUT1}	-0.665	0.104	-0.081	0.863
PUT1/CE versus DV _{PUT1} /DV _{CE}	0.944	0.001*	0.953	0.001*
PUT1/CE versus B _{max} /K _d (PUT1/CE)	0.948	0.001*	0.956	0.001*
DV _{PUT1} versus B _{max} /K _d (PUT1/CE)	-0.495	0.259	0.058	0.901
DV _{PUT1} /DV _{CE} versus B _{max} /K _d (PUT1/CE)	0.998	<0.0001*	0.996	<0.0001*
Putamen (with one ROI)				
PUT2/CE versus DV _{PUT2}	-0.724	0.066	-0.151	0.747
PUT2/CE versus DV _{PUT2} /DV _{CE}	0.936	0.002*	0.932	0.002*
PUT2/CE versus B _{max} /K _d (PUT2/CE)	0.943	0.001*	0.944	0.001*
DV _{PUT2} versus B _{max} /K _d (PUT2/CE)	-0.554	0.197	0.015	0.974
DV _{PUT2} /DV _{CE} versus B _{max} /K _d (PUT2/CE)	0.996	<0.0001*	0.994	<0.0001*

*Slope was significantly different from zero; p < 0.05.

CAU = caudate nucleus; CE = cerebellum; DV = distribution volume; PUT1 = whole putamen, with three small ROIs; PUT2 = whole putamen, with one large ROI.

icant correlations were observed when the occipital cortex was used as the nonspecific binding region (r = 0.912–0.994, p = <0.0001–0.0002). There was no correlation between plasma-input total DV values and any of the other measures (p > 0.05). However, the total DV values of the caudate or putamen correlated significantly with the total DV values of the occipital cortex or cerebellum (r = 0.907–0.971, p = 0.0001–0.0003 for the occipital cortex; and r = 0.815–0.964, p = 0.001–0.026 for the cerebellum).

DISCUSSION

The methods used in data analysis to assess the binding of SCH 23390 to dopamine D₁ receptors were all subject to errors from emission data measured by the PET camera and positioning. Our study showed that repeated SCH 23390 PET scans in normal subjects had a reliability ranging from 43% to 93%, depending on the method of analysis. Although the plasma-input DV method was more sensitive to between-subject variation (14.4%–18.5%) than other methods, it also had a high intraindividual variance (15.8%–16.6%), resulting in a very low reliability (43%–58%). All the other methods of analysis were less sensitive to between-subject variation (6.0%–11.3%), but they had a low intraindividual variance (2.3%–4.4%), leading to a high reliability (67%–95%). Of all the measures, tissue-input B_{max}/K_d with the cerebellum as the reference region had the highest reliability (88%–95%) in repeated scans, and plasma-input DV had the lowest reliability (43%–58%), although plasma-input DVRs had reliability measures nearly as high as the tissue-input B_{max}/K_d. The Logan plasma-input function method was subject to additional errors from blood data and metabolite analysis that, in turn, contributed to the poor reliability of the plasma-input DV. The ratio of metabolite to unchanged SCH 23390 in plasma increased with time in a linear relationship. However, the low reliability in the slopes (40%) reflected the variation in metabolite analysis and was probably due to the low counting rate of ¹¹C, especially for the 30- and 40-min samples analyzed after two half-lives, despite the use of a reliable HPLC method for metabolite analysis. Like the

caudate and putamen, the reliability of the DV values of the occipital cortex or cerebellum was also low (48%–56%). The reliability, however, improved substantially when plasma-input DVR rather than plasma-input total DV values were used. Similar findings with [¹¹C]raclopride have been shown by Logan et al. (9). The improved reliability of DVRs over total DV values could perhaps be explained by the existence of a strong correlation between the total DV values of the caudate or putamen and the DV values of the occipital cortex or cerebellum arising from their common dependence on the plasma input function.

The region used for nonspecific binding affected reliability. In this study, we used both the occipital cortex and cerebellum as reference regions in the calculation of radioactivity ratios and plasma-input DVRs. In addition, the radioactivity-time courses in both regions were used as tissue input function in Logan graphical analysis to obtain B_{max}/K_d. Although the data derived from both regions were highly correlated, the radioactivity ratios, plasma-input DVRs and tissue-input B_{max}/K_d were all higher when the cerebellum was used as the nonspecific binding region. This likely reflects the low density of dopamine receptors present in the cerebellum as compared to the cerebral cortical areas (10). Thus, the cerebellum has an advantage when a higher contrast of specific to nonspecific regions is needed, such as in disease states when dopamine D₁ receptor binding may be altered. Because the cerebellum is devoid of dopamine receptors, disease states, the aging process or other factors involving the dopamine receptors are also less likely to be a methodologic problem. Furthermore, the reliability for repeated scans was much higher (a difference of 6%–21%) when the cerebellum was used. Thus, the cerebellum would be more reliable than the occipital cortex as the reference region for SCH 23390. SCH 23390 is metabolized peripherally to O-sulfate and O-glucuronide conjugates (11), and these two polar, water-soluble metabolites are not likely to cross the blood-brain barrier. Therefore, in addition to the advantage of a very low density of dopamine receptors, the lack of radioactive metabo-

lites of SCH 23390 in the brain makes the cerebellum an ideal region for determination of free ligand and nonspecific binding.

Compartmental model fits of the reference tissue time courses were performed to provide the population mean values of the kinetic rate constants required for the tissue-input Logan analysis. The time courses in both the cerebellum and occipital cortex were fitted with a single-tissue compartment to reflect the assumption of negligible specific binding. Because of the small, but significant, specific binding in the occipital cortex, the calculation of Logan DVR values using this approach represents an approximation. Despite this, the correspondence between the DVR values derived from the tissue input method and those derived from the plasma input approach was seen to be nearly as good with the cortex as the reference tissue as with the cerebellum as the reference tissue.

Compartmental fits of the striatal time courses were also performed with two tissue compartments (free and nonspecifically bound ligand and specifically bound ligand) to test the assumption that the rates of equilibration between unbound ligand in plasma and tissue, and between bound and unbound ligand in tissue, were sufficiently rapid to justify the use of the graphical approaches. The goodness of fit, and the values of the fitted rate constants, strongly supported this assumption. This observation is consistent with the qualitative appearance of those data (Fig. 2); the gradual approach of the striatal and cerebellar time courses toward each other late in the study strongly implies that the binding of SCH 23390 is sufficiently reversible to justify the application of the Logan graphical approaches.

The size of the ROI had been shown to affect reliability of analysis for [¹⁸F]6-fluoro-L-DOPA (12). In this study, we had two different sets of ROIs placed on the putamen, one with three small ROIs and the other with one large ROI. Our results showed that the reliability of all the measures was slightly higher when three small ROIs instead of one large ROI were used. This may reflect inadvertent inclusion of receptor-poor regions when the larger ROI was used. This is particularly possible considering the anatomical shape of the putamen. Furthermore, all striatal regions were conservatively large in the axial direction, to assure that the entire striatum was included in all cases. This also may introduce a large fraction of nonspecific tissue into the regions that would otherwise be encountered, with a consequent bias of the estimated binding measures toward lower values.

CONCLUSION

The lack of correlation between plasma-input DV values and any of the other measures as well as the existence of a significant correlation between the DV values of the caudate or putamen and the DV values of the occipital cortex or cerebel-

lum suggest that DVRs rather than total DV values should be used for SCH 23390 when the Logan plasma-input function method is used. The significant correlations found among radioactivity ratios, plasma-input DVRs and tissue-input B_{\max}/K_d values indicate that all three are comparable and useful measures for the assessment of dopamine D₁ receptor binding. Also, these three measures are similar in terms of their sensitivity to distinguish between-subject and intrasubject variation. This suggests that, in the absence of reliable blood data, the radioactivity ratio method or the Logan tissue-input function method may be preferred for the evaluation of dopamine D₁ receptor binding because these two methods provide data with high reliability without the burden on the patients (invasiveness of arterial blood sampling) and blood and metabolite analysis. Carbon-11-SCH 23390 is a reliable and reproducible ligand for the study of dopamine D₁ receptor binding by PET.

ACKNOWLEDGMENTS

This work was supported by the Medical Research Council of Canada. We thank Edwin Mak and the TRIUMF PET group for their contribution to this work. We are also grateful to Dr. Allan Barnett of Schering Plough for supplying the precursor of SCH 23390.

REFERENCES

1. Farde L, Halldin C, Stone-Elander S, Sedvall G. PET analysis of human dopamine receptor subtypes using ¹¹C-SCH 23390 and ¹¹C-raclopride. *Psychopharmacology* 1987;92:278-284.
2. Suhara T, Fukuda H, Inoue O, Suzuki K, Yamasaki T, Tateno Y. Age-related changes in human D₁ receptors measured by positron emission tomography. *Psychopharmacology* 1991;103:41-45.
3. Farde L, Nordstrom AL, Wiesel F-A, Pauli S, Halldin C, Sedvall G. PET analysis of central D₁ and D₂ dopamine receptor occupancy in patients treated with classical neuroleptics and clozapine. *Arch Gen Psychiatry* 1992;49:538-544.
4. Shinotoh H, Inoue O, Hirayama K, et al. Dopamine D₁ receptors in Parkinson's disease and striatonigral degeneration: a positron emission tomography study. *J Neurol Neurosurg Psychiatry* 1993;56:467-472.
5. Logan J, Fowler J, Volkow N, et al. Graphical analysis of reversible radioligand binding from time-activity measurements applied to [N-¹¹C-methyl]-(-)-cocaine PET studies in human subjects. *J Cereb Blood Flow Metab* 1990;10:740-747.
6. Logan J, Fowler JS, Volkow ND, Wang G-J, Ding Y-S, Alexoff DL. Distribution volume ratios without blood sampling from graphical analysis of PET data. *J Cereb Blood Flow Metab* 1996;16:834-840.
7. Ravert HT, Wilson AA, Dannals RF, Wong DF, Wagner HN. Radiosynthesis of a selective dopamine D₁ receptor antagonist: R(+)-7-chloro-8-hydroxy-3-[¹¹C]methyl-1-phenyl-1,2,3,4,5-tetrahydro-1H-3-benzazepine ([¹¹C]SCH 23390). *Appl Radiat Isot* 1987;38:305-306.
8. Scheffe H. *The analysis of variance*. New York: Wiley and Sons; 1959:221-260.
9. Logan J, Volkow ND, Fowler JS, et al. Effects of blood flow on [¹¹C]raclopride binding in the brain: model simulations and kinetic analysis of PET data. *J Cereb Blood Flow Metab* 1994;14:995-1010.
10. Hall H, Sedvall G, Magnusson O, Kopp J, Halldin C, Farde L. Distribution of D₁- and D₂-dopamine receptors, and dopamine and its metabolites in the human brain. *Neuropsychopharmacology* 1994;11:245-256.
11. Swahn C-G, Halldin C, Farde L, Sedvall G. Metabolism of the PET ligand [¹¹C]SCH 23390. Identification of two radiolabelled metabolites with HPLC. *Hum Psychopharmacol* 1994;9:25-31.
12. Vingerhoets FJG, Snow BJ, Schulzer M, et al. Reproducibility of fluorine-18-6-fluorodopa positron emission tomography in normal human subjects. *J Nucl Med* 1994;35:18-24.